

## One- and Two-Dimensional CFAR Processors in the Presence of Strong Pulse Jamming<sup>1</sup>

*Ivan Garvanov, Christo Kabakchiev*

*Institute of Information Technologies, 1113 Sofia*

**Abstract:** *In this paper CA CFAR, excision CFAR, CA CFAR BI, excision CFAR BI and API CFAR processors in strong pulse jamming (PJ) are discussed . We investigate the influence of the scale factor over probability of false alarm and detection probability in strong PJ for one-dimensional CFAR processors. The efficiency of one- and two-dimensional CFAR processors by using the average decision threshold (ADT) approach is evaluated. The results for the ADT are received analytically using the Monte-Carlo method and the probability functions (SNR). The researches are performed in MATLAB environment.*

*The experimental results show that API CFAR processors are most efficient for probability of appearance of pulse jamming (from 0 up to 0.5). For  $\varepsilon_0 > 0.5$  we recommend binary integration after the CFAR processor.*

**Keywords:** *Radar Detector, CFAR Processors, Pulse Jamming, Average Decision Threshold (ADT), Probability of detection, Probability of false alarm.*

### 1. Introduction

Cell-Averaging Constant False Alarm Rate (CA CFAR) signal processing proposed by Finn and Johnson [1] is often used for radar signal detection. The detection

---

<sup>1</sup>This work is supported by IIT – BAS, No 010044, MPS Ltd. Grant “RDR” and Bulgarian NF “SR” Grant No I – 902/99.

threshold is determined as a product of the noise level estimate in the reference window and a scale factor to achieve the design probability of false alarm. The presence of strong pulse jamming (PJ) in both, the test resolution cell and the reference cells can cause drastic degradation in the performance of a CA CFAR processor as shown in [12].

In such situations it would be desirable to know the CFAR losses, depending on the parameters of PJ, for rating the behavior of radar. There are two approaches for the calculation of CFAR losses offered by R o l l i n g [2] and by G a n d h i and K a s s a m [3]. The conventional method, used in [5, 7, 12], is to compute the additional SNR needed for the CFAR processing scheme beyond that for the optimum processor, to achieve a fixed detection probability (e.g. 0.5). For a particular CFAR scheme the losses obviously vary with the detection probability. Alternatively, the authors in [2, 3] use another criterion based on the average decision threshold (ADT), since the threshold and the detection probability are closely related to each other. Then the difference between two CFAR systems is expressed by the ratio between the two ADTs measured in dB, as shown in [2, 3].

The false alarm rate of the postdetection integrator (PI) is extremely sensitive to pulse jamming, and the binary integrator (BI) which uses a K-out-of-M decision rule is insensitive to at most K-1 interfering pulses [7]. For keeping constant false alarm rate in PJ, the CA CFAR processor presented in [9, 12] is used. But this method is not as effective as the conventional method for the calculation of CFAR losses. For the minimization of CFAR losses in case of pulse jamming postdetection integration (PI) or binary integration (BI) is implemented in CFAR processors as shown in [5, 8, 10]. The use of excision CFAR detectors, supplemented by a postdetection integrator or a binary integrator as shown in [6, 7, 10], increases the CFAR losses. Minimum CFAR losses in PJ are obtained in [5, 11] with a CFAR adaptive postdetection integrator (API) processor with adaptive selection on PJ in reference windows and apriori selection in test windows as shown in [5] and adaptive censoring in reference and test windows as presented in [11].

We assume in this paper that the noise in the test cell is Rayleigh envelope distributed and target returns are fluctuating according to Swerling II model as in [3, 5]. Differing from the authors in [5], we assume that the samples of PJ are distributed according to the compound exponential law, where weighting coefficients are the probabilities of corrupting and non-corrupting of the samples. Differently from [7-11], we consider the entire range (from 0 up to 1) of the probability for the appearance of pulse jamming in range cells. For values of the weighting coefficients higher than 0.3, the Poisson process model is used, but it is rough [16]. The binomial distribution is correct in this case.

In this paper we research the influence of a scale factor over probability of false alarm, detection probability and average decision threshold in strong PJ for CA CFAR and excision CFAR processors. In [12] the losses of CA CFAR detector in conditions of PJ are calculated, but for fixed scale factor. In this case the probability of false alarm is not maintained constant.

In our work we study CA CFAR, excision CFAR, CFAR BI, excision CFAR BI and API CFAR processors in strong pulse jamming. We use the average decision

threshold (ADT) approach for comparison of the processors. As a difference from the authors in [7-11], we study the influence of probability for appearance of pulse jamming over ADT in strong PJ. The analytical expressions for the probability functions of CA CFAR, excision CFAR, CFAR BI, excision CFAR BI and API CFAR detectors are achieved in [7-11]. We achieve in this paper new results for the ADT of all studied by us CFAR processors using Rohling approach, presented in [2]. The SNR of the minimum detectable signal ( $P_D=0.5$ ) is approximately the same as the ADT of each CFAR system. We use for comparison also the approach with Monte-Carlo simulation for estimation of the ADT of the studied CFAR detectors. Finally, we estimate the efficiency of the CFAR processors by using the results for the ADT.

The experimental results show that the API CFAR processors are most effective for probability of appearance of pulse jamming (from 0 up to 0.5). For  $\varepsilon_0 > 0.5$  we recommend binary integration after the CFAR processor.

## 2. Performance of one-dimensional CA CFAR and excision CFAR processors in the presence of pulse jamming

### 2.1. Probability of detection and false alarm of CA CFAR detectors

Consider a radar detector in which the received signal is sampled in a range by the  $N + 1$  resolution cells resulting in a vector of  $N + 1$  observations. The sampling rate is such that the samples are statistically independent. After filtration the signal is applied to a square-law detector and then processed in the CA CFAR decision element. In conditions of pulse jamming the background environment includes random interfering pulses and the receiver noise. Therefore the samples surrounding the cell under test (a reference window) may be drawn from two classes. One class represents the interference-plus-noise situation, which may appear at the output of the receiver with a probability  $\varepsilon_0$ . This probability can be expressed as  $\varepsilon_0 = t_c F_j$ , where  $F_j$  is the average repetition frequency of PJ and  $t_c$  is the length of pulse transmission. The other class represents the noise only situation, which may appear at the outputs of the receiver with a probability  $(1 + \varepsilon_0)$ . The probability density function (pdf) of the test resolution cell is assumed to be distributed according to Swerling II case [9]:

$$(1) \quad f(x) = \frac{1 - \varepsilon_0}{\lambda_0(1 + s)} \exp\left(\frac{-x}{\lambda_0(1 + s)}\right) + \frac{\varepsilon_0}{\lambda_0(1 + r_j + s)} \exp\left(\frac{-x}{\lambda_0(1 + r_j + s)}\right),$$

where  $\lambda_0$  is the average power of the receiver noise,  $r_j$  is the average interference-to-noise ratio (INR) of pulse jamming,  $s$  is the per pulse average signal-to-noise ratio (SNR). The probability density function (pdf) of the reference window outputs can be defined as (1), setting  $s = 0$ .

The probability of pulse detection  $P_D$  is obtained in [9] as:

$$(2) \quad P_D = (1 - \varepsilon_0) M_V \left( \frac{T}{\lambda_0(1+s)} \right) + \varepsilon_0 M_V \left( \frac{T}{\lambda_0(1+r_j+s)} \right),$$

where  $M_V(\cdot)$  is the moment generating function (mgf) of the noise level estimate  $V$ . In a conventional CA CFAR detector the noise level estimate is formed as a sum of all the outputs of the reference window:  $V = \sum_{i=1}^N x_i$ . In this case the mgf of the estimate  $V$  is defined to be  $M_V(U) = M_x^N(U)$ , where  $M_x(U)$  is the mgf of the random variable  $x_i$ . The mgf of the estimate  $V$  is obtained in [9]:

$$(3) \quad M_V(U) = \sum_{i=1}^N \frac{C_N^i \varepsilon_0^i (1 - \varepsilon_0)^{N-i}}{(1 + \lambda_0 U)^{N-i} (1 + \lambda_0(1+r_j)U)^i}.$$

The probability of target detection in [9] is computed by the following expression:

$$(4) \quad P_D = \sum_{i=1}^N C_N^i \varepsilon_0^i (1 - \varepsilon_0)^{N-i} \left\{ \frac{\varepsilon_0}{\left(1 + \frac{(1+r_j)T}{1+r_j+s}\right)^i \left(1 + \frac{T}{1+r_j+s}\right)^{N-i}} + \frac{1 - \varepsilon_0}{\left(1 + \frac{(1+r_j)T}{1+s}\right)^i \left(1 + \frac{T}{1+s}\right)^{N-i}} \right\}.$$

The probability of false alarm is evaluated by (4), setting  $s = 0$ .

## 2.2. Probability of detection and false alarm of excision CFAR detectors

In an excision CFAR processor the noise level estimate  $V$  is formed as an average mean of nonzero samples at the output of the excisor  $\{y_i\}_N$ , that is:  $V = \frac{1}{k} \sum_{i=1}^K y_i$ . According to [6] the operation of the excisor is defined as follows:

$$(5) \quad y_i = \begin{cases} x_i & \text{if } x_i \leq B_E, \\ 0 & \text{otherwise,} \end{cases}$$

where  $B_E$  is the excision threshold.

Therefore the pdf of the random variable  $y_i$  can be expressed as

$$(6) \quad f(y_i) = \frac{(1 - \varepsilon_0) \exp\left(\frac{-y_i}{\lambda_0}\right)}{\lambda_0 \left(1 - \exp\left(\frac{-B_E}{\lambda_0}\right)\right)} + \frac{\varepsilon_0 \exp\left(\frac{-y_i}{\lambda_0(1+r_j)}\right)}{\lambda_0(1+r_j) \left(1 - \exp\left(\frac{-B_E}{\lambda_0(1+r_j)}\right)\right)}.$$

The probability that a sample  $x_i$  survives at the output of the excisor, is given as

$$(7) \quad P_E = 1 - (1 - \varepsilon_0) \exp\left(\frac{-B_E}{\lambda_0}\right) - \varepsilon_0 \exp\left(\frac{-B_E}{\lambda_0(1+r_j)}\right).$$

The probability that  $k$  out of  $N$  samples of the reference window survive at the output of the excisor is given as:  $\nu(k) = C_N^k P_E^k (1 - P_E)^{N-k}$ . The mgf of the random variable  $y_i$  at the output of the excisor can be obtained using the following expression:

$$(8) \quad M_y(U) = \frac{\varepsilon_0 (1 - \exp(R_1 - B_E U))}{(1 - \exp(R_1))(1 + U\lambda_0(1+r_j))} + \frac{(1 + \varepsilon_0)(1 - \exp(R_2 - B_E U))}{(1 - \exp(R_2))(1 + U\lambda_0)},$$

$$\text{where } R_1 = \frac{-B_E}{\lambda_0(1+r_j)}; \quad R_2 = \frac{-B_E}{\lambda_0}.$$

Since the random variables  $x_i (1 \leq i \leq k)$  are independent, the mgf of the estimate  $V$  can be obtained as a product:  $M_V(U, k) = M_Y^k(U/k)$ . In this article we use the moment generating function on the excision CFAR processor from [7]

$$(9) \quad M_V(U) = \sum_{k=1}^N C_N^k P_E^k (1 - P_E)^{N-k} M_V(U, k),$$

where

$$(10) \quad M_V(U, k) = \sum_{i=0}^k C_k^i \left\{ \frac{\varepsilon_0 (1 - \exp(R_1 - B_E U/k))}{(1 - \exp(R_1))(1 + U\lambda_0(1+r_j)/k)} \right\}^i \left\{ \frac{(1 + \varepsilon_0)(1 - \exp(R_2 - B_E U/k))}{(1 - \exp(R_2))(1 + U\lambda_0/k)} \right\}^{k-i}$$

The probability of target detection for excision CFAR in [7] is computed by the expression:

$$(11) \quad P_D = \sum_{k=1}^N C_N^k P_E^k (1 - P_E)^{N-k} \left\{ (1 - \varepsilon_0) M_V\left(\frac{T}{\lambda_0(1+s)}, k\right) + \varepsilon_0 M_V\left(\frac{T}{\lambda_0(1+r_j+s)}, k\right) \right\}.$$

The probability of false alarm is evaluated by (11), setting  $s = 0$ .

2.3. Average decision threshold of CA CFAR and excision CFAR detectors  
The average decision threshold ADT is defined as a normalized quantity [2]:

$$(12) \quad \text{ADT}_{\text{CFAR}} = E(TV) / \lambda_0,$$

where the random variable  $V$  is the result of the estimation method used in the CFAR system,  $T$  is the scaling factor for threshold adjustment adapted to the estimation method and required  $P_{FA}$ ;  $E$  stands for the expectation:

$$(13) \quad E(V) / \lambda_0 = -\frac{d}{dT} M_V \left( T / \lambda_0 \right) \Big|_{T=0}.$$

Deviating from the methods usually described in radar literature, we use the average decision threshold (ADT) for comparison of various CFAR processors. This provides the advantage that the difference existing between various CFAR systems is then expressed by a single-valued measure. The difference between two CFAR systems can be expressed by the ratio of the two ADT's measured in dB [2]:

$$(14) \quad \Delta = \frac{\text{ADT}_1}{\text{ADT}_2} = 10 \log \frac{E(T_1 V_1)}{E(T_2 V_2)} \quad \text{for} \quad P_{fa1} = P_{fa2}, \quad P_{D1} = P_{D2} = 0.5.$$

In this paper comparative analysis by ADT for one dimension processors is made with respect to an optimal detector, as it is in [3]. The ATD optimal is

$$(15) \quad \text{ADT}_{\text{opt}} = -\ln(P_{fa}).$$

**2.3.1. ADT for a CA CFAR processor in PJ.** Using (3) and (13), we substitute  $U = T / \lambda_0$  and for  $T = 0$ , we have the ADT expression as it is in [12]:

$$(16) \quad \text{ADT}_{\text{CACFAR}} = T \frac{E(V)}{\lambda_0} = T \left( -\frac{d}{dT} M_V \left( \frac{T}{\lambda_0} \right) \Big|_{T=0} \right) = T \sum_{i=0}^N C_N^i \varepsilon_0^i (1 - \varepsilon_0)^{N-i} (N + ir_j),$$

where  $T$  is computed by expression (4), setting  $s = 0$ .

For  $\varepsilon_0 = 0$  or without pulse jamming  $\text{ADT}_{\text{CACFAR}} = TN$  as in [3], where  $T = (P_{fa})^{-1/N} - 1$ .

**2.3.2. ADT for excision CFAR processor in PJ .** Using (9) and (13), we substitute  $U = T / \lambda_0$  and for  $T = 0$ , we have the ADT expression as it is in [13]:

$$\begin{aligned}
\text{ADT}_{\text{EXCCFAR}} = & -T \sum_{k=1}^N C_N^k P_E^k (1 - P_E)^{N-k} \left\{ \sum_{i=0}^k C_k^i \left[ \frac{\varepsilon_0}{(1 - \exp(R_1))} \right]^i \left[ \frac{(1 - \varepsilon_0)}{(1 - \exp(R_2))} \right]^{k-i} \right. \\
(17) \quad & \times \frac{1}{\lambda_0 k} \left\{ (1 - \exp(R_1))^{i-1} \left[ \exp(R_1)(B_E + \lambda_0(1 + r_j)) - \lambda_0(1 + r_j) \right] (1 - \exp(R_2))^{k-i} + \right. \\
& \left. \left. + (k - i)(1 - \exp(R_2))^{k-i-1} \left[ \exp(R_2)(B_E + \lambda_0) - \lambda_0 \right] (1 - \exp(R_1))^i \right\} \right\},
\end{aligned}$$

where  $T$  is computed by expression (11) setting  $s = 0$ .

### 3. Performance of two-dimensional CFAR BI, excision CFAR BI and API CFAR processors in the presence of pulse jamming.

Let us assume that  $L$  pulses hit the target, which is modeled according to Swerling case II. The received signal is sampled in range by using  $M + 1$  resolution cells resulting in a matrix with  $M + 1$  rows and  $L$  columns. Each column of the data matrix consists of the values of the signal obtained for  $L$  pulse intervals in one range resolution cell. Let us also assume that the first  $M / 2$  and the last  $M / 2$  rows of the data matrix are used as a reference window in order to estimate the “noise-plus-interference” level in the test resolution cell of the radar. In this case the samples of the reference cells result in a matrix  $X$  of the size  $M \times L$ . The test cell or the radar target image includes the elements of the  $(M / 2 + 1)$  row of the data matrix and is a vector  $Z$  of length  $L$ . The elements of the reference window are independent random variables with compound exponential distribution law (1), setting  $s = 0$ . In the presence of a desired signal from a target the elements of the test resolution cell are independent random variables with distribution law (1).

#### 3.1. Probability of detection and false alarm of CA CFAR BI detectors

The probability of target detection for CA CFAR BI processor in [10] is computed by the expression

$$(18) \quad P_{D_i} = \sum_{l=M}^L C_L^l P_D^l (1 - P_D)^{L-l},$$

where  $P_D$  is probability of detection from (4). The probability of false alarm is evaluated by (18), setting  $s = 0$ .

#### 3.2. Probability of detection and false alarm of excision CFAR BI detectors

The probability of target detection for EXC CFAR BI processor in [10] is computed by the expression

$$(19) \quad P_{D_2} = \sum_{l=M}^L C_L^l P_D^l (1 - P_D)^{L-l},$$

where  $P_D$  is probability of detection from (11). The probability of false alarm is evaluated by (19), setting  $s = 0$ .

### 3.3. Probability of detection and false alarm of API CFAR detectors

We use the adaptive censoring algorithm, proposed by H i m o n a s and B a r k a t in [4], before pulse-to-pulse integration for censoring the elements of pulse jamming in the reference window and the test resolution cells, in order to form the detection algorithm.

The expression for the probability of target detection for an API CFAR processor is achieved in [11, 15]. The authors in [11, 15] study the probability of target detection only for  $\varepsilon_0 \leq 0.5$  and calculate only the first member of the expression (20). We calculate the probability of target detection for  $\varepsilon_0 \in (0; 1)$  and calculate the value of  $P_D$  by using the following expression:

$$(20) \quad \begin{aligned} P_D = & \sum_{k=1}^N \binom{N}{k} (1 - \varepsilon_0)^k \varepsilon_0^{N-k} \sum_{l=1}^L \binom{L}{l} (1 - \varepsilon_0)^l \varepsilon_0^{L-l} \sum_{i=0}^{l-1} \binom{k+i-1}{i} \frac{T^i (1+s)^k}{(T+1+s)^{k+i}} + \\ & + \sum_{k=1}^N \binom{N}{k} (1 - \varepsilon_0)^k \varepsilon_0^{N-k} \varepsilon_0^L \sum_{i=0}^{L-1} \binom{k+i-1}{i} T^i (1+r_j+s) (T+1+r_j+s)^{(k+i)} + \\ & + \sum_{l=1}^L \binom{L}{l} (1 - \varepsilon_0)^l \varepsilon_0^{L-l} \varepsilon_0^N \sum_{i=0}^{l-1} \binom{N+i-1}{i} T^i \left( \frac{1+s}{1+r_j} \right)^N \left( T + \frac{1+s}{1+r_j} \right)^{-(N+i)} + \\ & + \varepsilon_0^N \varepsilon_0^L \sum_{i=0}^{L-1} \binom{N+i-1}{i} T^i \left( \frac{1+r_j+s}{1+r_j} \right)^N \left( T + \frac{1+r_j+s}{1+r_j} \right)^{-(N+i)} \end{aligned}$$

## 4. Numerical results

### 4.1. Scale factor analysis of CA CFAR and excision CFAR detectors in pulse jamming

In this paper we investigate the influence of scale factor over probability of false alarm and detection probability in strong PJ for CA CFAR and excision CFAR processors. We use the scale factor  $T_c = f(P_{fa}, N) = 1.3713$  for the case of homogeneous interference and  $T_p = f(P_{fa}, N, r_j, \varepsilon_0)$  for the case when the false alarm probability is maintained constant in pulse jamming. The experimental results are obtained for the following parameters: average power of the receiver noise  $\lambda_0 = 1$ , average interference-to-noise ratio (INR)  $r_j = 5$  and 30 dB, probability for appearance of pulse jamming with average length in the range cells  $\varepsilon_0$  from 0 to 1, number of reference cells  $N = 16$ , probability of false alarm  $P_{fa} = 10^{-6}$  and excision threshold  $B_E = 2$ .



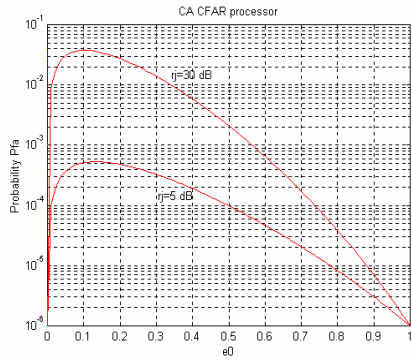


Fig. 1. CA CFAR processor.  
False alarm probability for  $T_c$

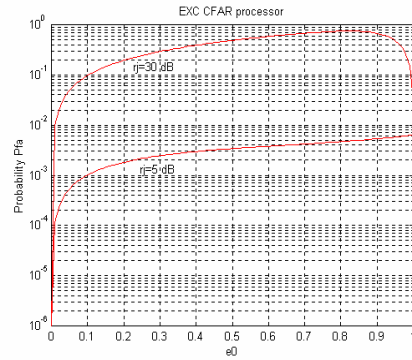


Fig. 2. EXC CFAR processor.  
False alarm probability for  $T_c$

The experimental results from Fig.1 and 2 show that when CA CFAR and excision CFAR processors operate with fixed scale factor  $T_c$  in strong pulse jamming the false alarm probability is not maintained constant. In this case the detection probability decrease with increase of the average interference-to-noise ratio and the probability for the appearance of pulse jamming with average length in the range cells for fixed SNR (Figs. 3-6). For case with adaptive scale factor  $T_p$  threshold ratio SNR is bigger for fixed the detection probability  $P_d = 0.5$ .

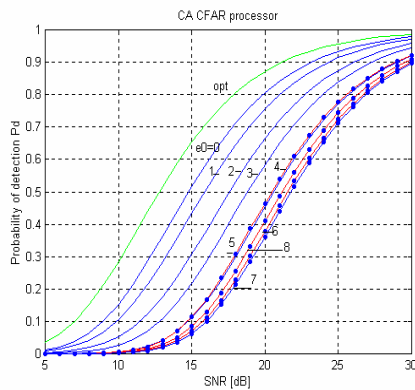


Fig. 3. CA CFAR processor.  
Detection probability for  $r_j=5$  dB and  $\epsilon_0=0.1, 0.3, 0.5, 0.9$ , where  $\epsilon_0$  is 1, 2, 3, 4 for  $T_c$  and 5, 6, 7, 8 for  $T_p$

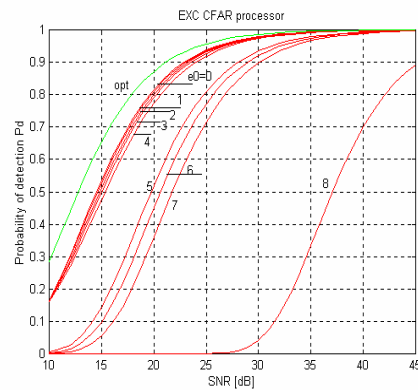


Fig. 4. EXC CFAR processor.  
Detection probability for  $r_j=5$  dB and  $\epsilon_0=0.1, 0.3, 0.5, 0.9$ , where  $\epsilon_0$  is 1, 2, 3, 4 for  $T_c$  and 5, 6, 7, 8 for  $T_p$

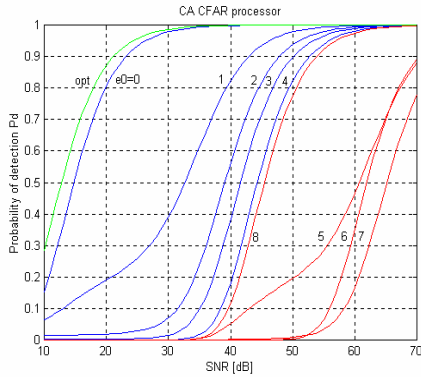


Fig. 5. CA CFAR processor.

Detection probability for  $r_j=30$  dB and  $\varepsilon_0=0.1, 0.3, 0.5, 0.9$ , where  $\varepsilon_0$  is 1, 2, 3, 4 for  $T_c$  and 5, 6, 7, 8 for  $T_p$

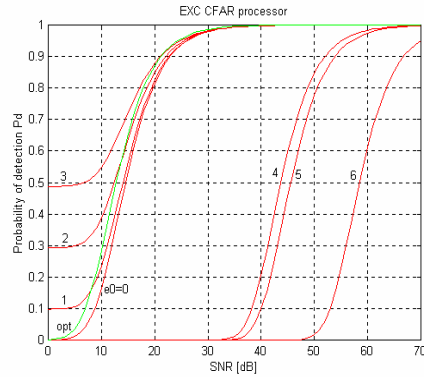


Fig. 6. EXC CFAR processor.

Detection probability for  $r_j=30$  dB and  $\varepsilon_0=0.1, 0.3, 0.5$ , where  $\varepsilon_0$  is 1, 2, 3 for  $T_c$  and 4, 5, 6 for  $T_p$

#### 4.2. Average decision threshold analysis of one-dimensional CFAR processors in PJ

In a CA CFAR processor, the noise level estimate in the reference window increases with the increasing of the average interference-to-noise ratio and the probability for the appearance of pulse jamming with average length in the range cells (Fig.7). In order to keep the false alarm probability constant, the scale factor must be decreased when the PJ frequency increases. The average decision threshold (ADT) increases when the probability for the appearance of pulse jamming takes values  $\varepsilon_0$  from 0 to 0.5, and then decreases for value  $\varepsilon_0 > 0.5$  (Fig. 7).

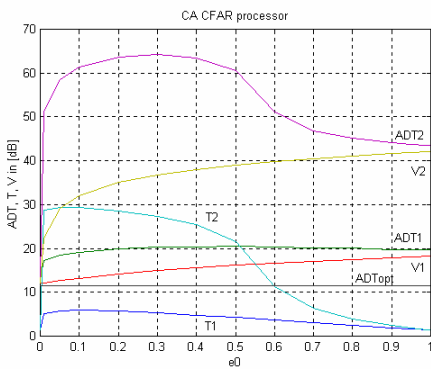


Fig. 7. CA CFAR processor.  
ADT1, T1, V1 and ADT2, T2, V2  
are for  $r_j=5$  and 30 dB

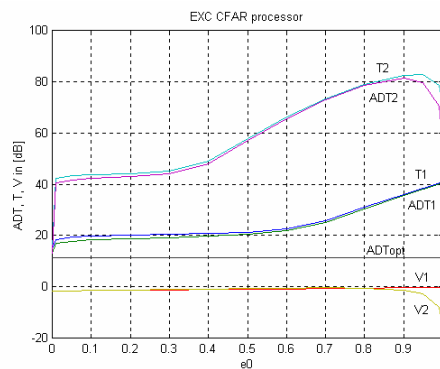


Fig. 8. EXC CFAR processor.  
ADT1, T1, V1 and ADT2, T2, V2  
are for  $r_j=5$  and 30 dB

In the excision CFAR processor, the jamming pulses are censored and the noise level estimate in the reference window is kept constant (Fig.8). In order to keep the false

alarm probability constant, the scale factor must be increased with the increasing of PJ frequency. The average decision threshold (ADT) is constant when the probability for the appearance of pulse jamming takes values  $\varepsilon_0$  between 0 and 0.5, and then increases for a value  $\varepsilon_0 > 0.5$  (Fig.8).

In (Figs. 9 and 10) we present plots of the losses of CA CFAR and excision CFAR processors with relation to an optimal detector and losses in conditions of strong pulse jamming for average interference-to-noise ratio 5 and 30 dB. The difference between two CFAR systems is expressed by their losses, which are calculated with the help of expression (12). From (Figs.9 and 10) we show that excision CFAR processor is effective for probability of appearance of pulse jamming  $\varepsilon_0 \leq 0.5$ , for  $\varepsilon_0 > 0.5$  CA CFAR processor operates better.

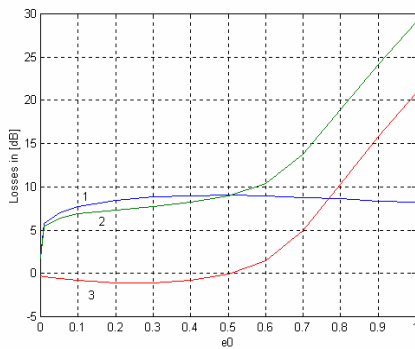


Fig. 9.  $r_j=5$  dB.

1 and 2 are losses of CA CFAR and EXC CFAR processors towards optimal detector 3 losses of EXC CFAR toward CA CFAR processor

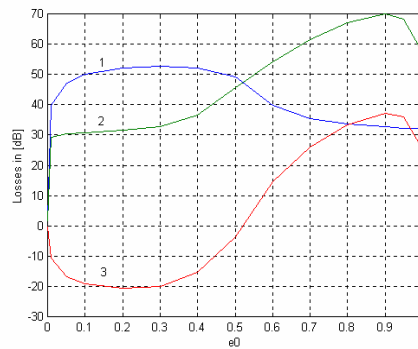


Fig. 10.  $r_j=5$  dB.

1 and 2 are losses of CA CFAR and EXC CFAR processors towards optimal detector 3 losses of EXC CFAR toward CA CFAR processor

In this paper we study average decision threshold in PJ for CA CFAR and excision CFAR processors with different methods. The results for ADT are analytically received using Monte-Carlo method and the probability functions (SNR). They are marked as follows: analytical (—), Monte-Carlo (\*) and SNR (continuous line). The experimental results are obtained for interference-to-noise ratio (INR)  $r_j=30$  dB.

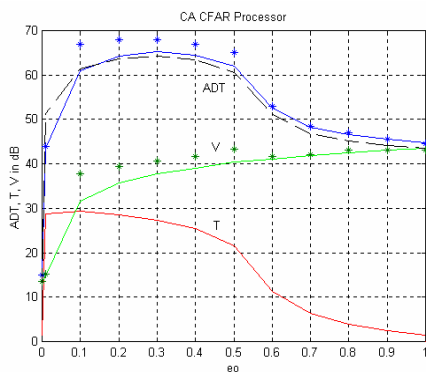


Fig. 11. CA CFAR processor

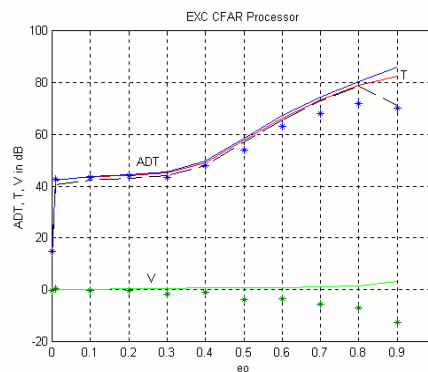


Fig. 12. EXC CFAR processor

It can be seen in Fig.11 and Fig.12 that the results achieved for ADT analytically and by using the probability functions (SNR) are identical, which proves the hypothesis of Rohling in [2]. All the above-mentioned allows us to determine the ADT of two-dimensional detectors by using the probability functions (SNR).

#### 4.3. Average decision threshold analysis of two-dimensional CFAR processors in PJ

The experimental results are obtained for the following parameters: average power of the receiver noise  $\lambda_0=1$ , average interference-to-noise ratio (INR)  $r_f=30$  dB, probability for the appearance of pulse jamming with average length in the range cells  $\varepsilon_0$  from 0 to 1, probability of false alarm  $P_{fa}=10^{-6}$  and excision threshold  $B_E=2$ . For two-dimensional detectors the size of the testing sample is 16 and the reference window is of the size  $16 \times 16$ . The results for the ADT are received using Monte-Carlo method and the probability functions (SNR). They are marked as follows: Monte-Carlo (\*) and SNR (continuous line).

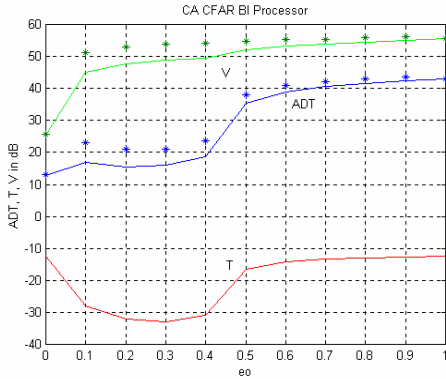


Fig. 13. CA CFAR BI processor,  $M=16, L=16$

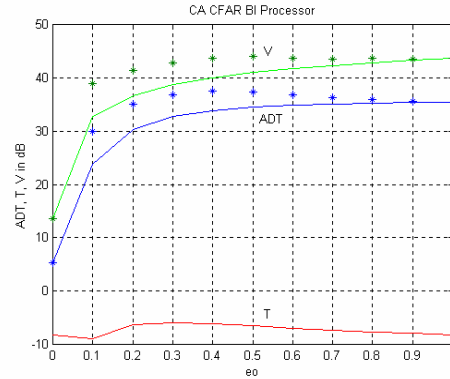


Fig. 14. CA CFAR BI processor,  $M=10, L=16$

The ADT, T and V of CA CFAR BI processors with a binary rule  $M$ -out-of- $L$  (16/16 and 10/16) are shown in Fig.13 and Fig.14. It can be seen that CFAR BI processors with the binary rule  $M$ -out-of- $L=16/16$  are better in cases of lower values  $\varepsilon_0 \leq 0.5$  of the probability for appearance of pulse jamming. For higher values of the probability for appearance of pulse jamming  $\varepsilon_0 > 0.5$  the using of the binary rule  $M$ -out-of- $L=10/16$  results in lower losses.

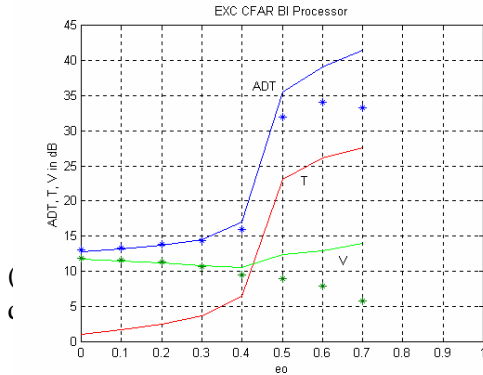


Fig. 15. EXC CFAR BI processor,  $M=16, L=16$

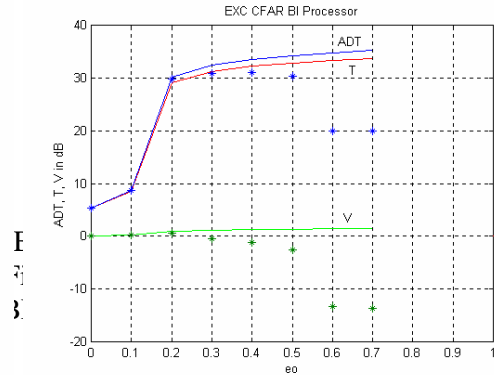


Fig. 16. EXC CFAR BI processor,  $M=10, L=16$

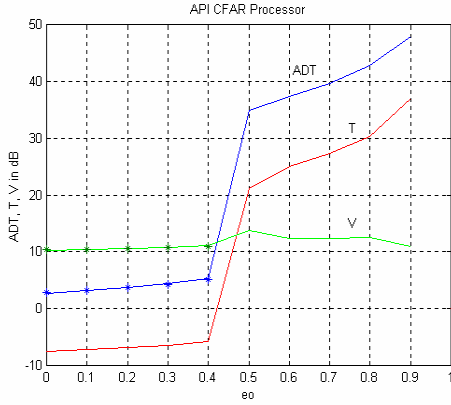


Fig. 17. API CFAR processor

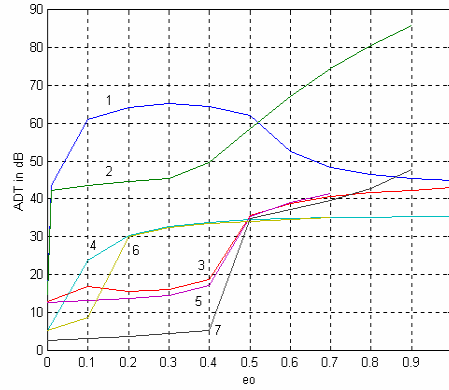


Fig. 18. ADT from Fig.11 up to Fig.17

The ADT,  $T$  and  $V$  of an API CFAR processor are shown in Fig.17. In this case the results for the ADT achieved by using the probability functions (SNR) are identical with the results achieved by using Monte-Carlo simulation for values of  $\varepsilon_0$  up to 0.4. The suggested algorithm is not working for higher values of  $\varepsilon_0$  due to the fact, that the hypothesis for censoring in the test cell is disturbed. In such case the big difference in power between the background and the pulse jamming is disturbed and the automatic censoring of pulse jamming is impossible.

The ADTs of all processors studied are shown in Fig.18. The numbers from 1 up to 7 correspond to the detectors from Fig.11 up to Fig.17. The API CFAR processor is the most suitable one to use for values of the probability for the appearance of pulse jamming  $\varepsilon_0 \leq 0.5$ . When the probability for the appearance of pulse jamming  $\varepsilon_0$  takes a value between 0.5 and 1, both CA CFAR BI and EXC CFAR BI processors with M-out-of-L=10/16 rule can be successfully used.

## 5. Conclusions

We investigate in this paper the technical qualities of different CFAR techniques in the presence of strong pulse jamming by using the ADT approach suggested by Rohling. We consider the whole range (from 0 up to 1) of the probability for appearance of pulse jamming in range cells. The ADTs are determined using analytical expressions, probability functions and Monte-Carlo simulation.

In this paper we investigate the influence of the scale factor over probability of false alarm, detection probability and average decision threshold in strong PJ for CA CFAR and excision CFAR processors. When CA CFAR and excision CFAR detectors operate with a fixed scale factor, the detection probability is decreased in strong PJ, but the false alarm probability is not maintained constant. When the scale factor is adjusted to PJ so that the false alarm probability is maintained constant, as it in our case, the ADT for CA CFAR processor increases with the increasing of the average interference-to-noise ratio  $r_j$  and the probability for the appearance of pulse jamming with average length in the

range cells from  $\varepsilon_0$  up to 0.5. The results obtained for the ADT of a CA CFAR processor without pulse jamming are equal to those presented in [3]. It can be seen from the experimental results that excision CFAR processor is effective for probability for appearance of pulse jamming  $\varepsilon_0 \leq 0.5$ , for  $\varepsilon_0 > 0.5$  CA CFAR processor operates better. For pulse jamming with probability for appearance of pulse jamming from 0.2 up to 0.3 and average interference-to-noise ratio  $r_j = 30$  dB, the profit from the excision is about 20 dB, and for  $r_j = 5$  dB the profit is about 2 dB.

The experimental results from the study on two-dimensional CFAR processors, show that API CFAR processors are most suitable for use when the probability for appearance of pulse jamming takes values in the interval from 0 up to 0.5. In cases when the probability for appearance of pulse jamming takes values in the interval from 0.5 up to 1, we recommend binary integration after the CFAR processor.

The problem, concerning the improvement of the work of excision CFAR and API CFAR processors when the probability for appearance of pulse jamming takes values in the interval  $\varepsilon_0 > 0.5$ , can be solved using H i m o n a s [5] approach. In such cases the threshold estimation is achieved using cells with pulse jamming.

## References

1. F i n n, H. M., P. S. J o h n s o n. Adaptive detection mode with threshold control as a function of spatially sampled clutter estimation. – RCA Review, **29**, 1968, No 3, 414-464.
2. R o h l i n g, H. Radar CFAR Thresholding in clutter and multiple target situations. – IEEE Trans., **AES-19**, 1983, No 4, 608-621.
3. G a n d h i, P. P., S. A. K a s s a m. Analysis of CFAR processors in nonhomogeneous background. – IEEE Trans., **AES-24**, 1988, No 4, 443-454.
4. H i m o n a s, S., M. B a r k a t. Automatic censored CFAR detection for nonhomogeneous environments. – IEEE Trans., **AES-28**, 1992, No 1, 286-304.
5. H i m o n a s, S. CFAR Integration processors in randomly arriving impulse interference. – IEEE Trans., **AES-30**, 1994, No 3, 809-816.
6. G o l d m a n, H. Analysis and application of the excision CFAR detector. – IEE Proceedings, **135**, 1988, No 6, 563-575.
7. B e h a r, V., C. K a b a k c h i e v. Excision CFAR binary integration processors. – Compt. Rend. Acad. Bulg. Sci., **49**, 1996, No 11/12, 45-48.
8. K a b a k c h i e v, C., V. B e h a r. CFAR radar image detection in pulse jamming. – In: IEEE Fourth Int. Symp. ISSSTA'96, Mainz, Germany, 1996, 182-185.
9. B e h a r, V. CA CFAR radar signal detection in pulse jamming. – Compt. Rend. Acad. Bulg. Sci., **49**, 1996, No 7/8, 57-60.
10. K a b a k c h i e v, C., V. B e h a r. Techniques for CFAR radar image detection in pulse jamming. – In: IEEE Fourth Int. Symp. EUM'96, Praga, Czech Republic, 1996, 347-352.
11. B e h a r, V., C. K a b a k c h i e v, L. D u k o v s k a. Adaptive CFAR processor for radar target detection in pulse jamming. – Journal of VLSI Signal Processing, **26**, 2000, No 11/12, 383-396.
12. K a b a k c h i e v, C., L. D u k o v s k a, I. G a r v a n o v. Comparative analysis of losses of CA CFAR processors in pulse jamming. – CIT, 2001, No 1, 21-35.
13. G a r v a n o v, I., C. K a b a k c h i e v. Average decision threshold of CA CFAR and excision CFAR detectors in the presence of strong pulse jamming. – In: German Radar Symposium 2002, (GRS 2002). Bonn, Germany, September, 2002, (submitted for print).
14. G a r v a n o v, I., V. B e h a r, C. K a b a k c h i e v. CFAR processors in pulse jamming. – In: Conference "Numerical Methods and Applications – NM&A02, August 20 - 24, 2002, Borovets, Bulgaria (submitted for print).

15. C h a k a r o v, V. Adaptive CFAR processor for radar target detection design of SHARC signal processor. Ph. D thesis, Technical University – Sofia, 1999.
16. A c h i m o v, P., P h. E v s t r a t o v, S. Z a h a r o v. Radiosignals detection. Moscow, Radio i sviaz, 1989.

## Едномерни и двумерни процесори, поддържащи постоянна честота на лъжлива тревога в условията на хаотични импулсни смущения

*Иван Гарванов, Христо Кабакчиев*

*Институт по информационни технологии, 1113 София*

### (Резюме)

В настоящата статия се изследват CA CFAR, excision CFAR, CA CFAR VI, excision CFAR VI и API CFAR процесори в условия на импулсни смущения. Изследва се влиянието на скаларния фактор върху вероятността за лъжлива тревога и вероятността на правилно откриване за едномерни процесори, поддържащи постоянна честота на лъжлива тревога. Оценява се ефективността на едномерните и двумерните откриватели, използвайки метода със среден праг на откриване. Резултатите за този праг са получени посредством аналитично извеждане, чрез симулация Монте - Карло и посредством използването на вероятностните функции на откривателите. Изследванията са направени в средата на MATLAB.

От получените резултати се вижда, че API CFAR процесорите са най-ефективни в условията на хаотични импулсни смущения при вероятност за тяхната поява от 0 до 0,5. За вероятност за поява, по-голяма от 0,5, се предлага използването на бинарно интегриране след процесорите, поддържащи постоянна честота на лъжлива тревога.